Hindawi Publishing Corporation
Advances in High Energy Physics
Volume 2016, Article ID 1760219, 12 pages
http://dx.doi.org/10.1155/2016/1760219

Hindawi

Research Article

Effects of the FCNC Couplings in Production of New Heavy Quarks within Z' Models at the LHC

V. Çetinkaya,[1] V. Arı,[2] and O. Çakır[2]

[1]*Department of Physics, Dumlupinar University, Merkez, 43100 Kutahya, Turkey*
[2]*Department of Physics, Ankara University, Tandogan, 06100 Ankara, Turkey*

Correspondence should be addressed to V. Çetinkaya; volkan.cetinkaya@dpu.edu.tr

Received 30 December 2015; Revised 20 March 2016; Accepted 3 May 2016

Academic Editor: Michal Kreps

We study the flavor changing neutral current couplings of new heavy quarks through the Z' models at the LHC. We calculate the cross sections for the signal and the corresponding standard model background processes. Considering the present limits on the mass of new heavy quarks and the Z' boson, we performed an analysis to investigate the parameter space (mixing and mass) through different Z' models. For FCNC mixing parameter $x = 0.1$ and the Z' mass $M_{Z'} = 2000$ GeV and new heavy quark mass $m_{t'} = 700$ GeV at the LHC with $\sqrt{s} = 13$ TeV, we find the cross section for single production of new heavy quarks associated with top quarks as 5.8 fb, 3.3 fb, 1.5 fb, and 1.2 fb within the Z'_η, Z'_ψ, Z'_{LP}, and Z'_χ models, respectively. It is shown that the sensitivity would benefit from the flavor tagging.

1. Introduction

Addition of new heavy quarks would require the extension of the flavor mixing in charged current interactions as well as the extension of Higgs sector in the standard model (SM). A large number of new heavy quark pairs can be produced through their color charges at the Large Hadron Collider (LHC). However, due to the expected smallness of the mixing between the new heavy quarks and known quarks through charged current interactions, the production and decay modes can be affected by the flavor changing neutral current (FCNC) interactions. A new symmetry beyond the SM is expected to explain the smallness of the mixing. We may anticipate the new physics discovery by observing large anomalous couplings in the heavy quark sector. The couplings of the new heavy quarks can be enhanced to observable levels within some new physics models. In numerous phenomenological studies (see [1] and references therein), a lot of extensions of the SM foresee the extra gauge bosons, the Z' boson in particular. Flavor changing neutral currents can be induced by an extra $U(1)'$ gauge boson Z'. The Z' boson in the models using an extra $U(1)'$ group can have tree-level or an effective $Z'q\bar{q}'$ (where q and q' both can be the up-type quarks or down-type quarks) couplings. The Z'_η, Z'_χ, and Z'_ψ models corresponding to the specific values of the mixing angle in the E_6 model with different couplings to the fermions and the leptophobic Z'_{LP} model with the couplings to quarks but no couplings to leptons are among the special names of the Z' models [2].

The ATLAS and CMS collaborations have performed extensive searches of new vector resonances at the LHC. We summarize briefly these searches that exploited data from the pp run at $\sqrt{s} = 7$ TeV and $\sqrt{s} = 8$ TeV, as well as the corresponding constraints on Z' boson masses. The most stringent limits come from searches with leptonic final states ($Z' \to l^+l^-$): $M_{Z'_\chi} > 2620$ GeV [3] and $M_{Z'_\eta} > 1870$ GeV [4], $M_{Z'_\psi} > 2260$ GeV [5] (more recently $M_{Z'_\psi} > 2510$ GeV [3]) for the Z' boson predicted by the $U(1)'$ extensions, also extending to the mass limit of $M_{Z'_s} > 2900$ GeV [3, 6] for a gauge boson with sequential couplings. The results from ATLAS experiment exclude a leptophobic Z' decaying to $t\bar{t}$ with a mass less than 1740 GeV at 95% CL [7], while the CMS experiment excludes a top-color Z' decaying to $t\bar{t}$ with a mass

less than 2100 GeV at 95% CL [8]. These searches assume rather narrow width for the Z' boson ($\Gamma_{Z'}/M_{Z'} = 0.012$). From the electroweak precision data analysis, the improved lower limits on the Z' mass are given in the range 1100–1500 GeV, which gives a limit on the Z–Z' mixing about 10^{-3} [2]. The limits on the Z' boson mass favors higher center of mass energy collisions for direct observation of the signal. Using dilepton searches with LHC data, the dark matter constraints have been analyzed in [9, 10] in the regime $M_{Z'} > 2m_{\mathrm{DM}}$.

A work performed in [11, 12] presents the effects of FCNC interactions induced by an additional Z' boson on the single top quark and top quark pair production at the LHC ($\sqrt{s} = 14$ TeV). The relevant signal cross sections have been calculated and particularly the benefit from flavor tagging to identify the signal has been discussed. Considering an existence of sizeable couplings to the new heavy quarks, the Z' boson decay width and branchings, as well as the production rates, can be quite different from the expectations of usual search scenarios.

In the models of interest new heavy quarks can have some mixing with the SM quarks. For example, in composite Higgs model [13] the lightest new heavy quark couples predominantly to the heavier SM quarks (top and bottom quarks). In the models of vector-like quarks (VLQ) [14] they are expected to couple preferentially to third-generation quarks and they can have flavor changing neutral current couplings, in addition to the charged current decays characteristic of chiral quarks. Within the E_6 model the isosinglet quarks [15] are predicted and they can decay to the quarks of the SM. The new heavy quarks can be produced dominantly in pairs through strong interactions for masses around 1 TeV in the pp collisions of the LHC with a center of mass energy of 13 TeV. The single production of new heavy quarks would only be dominant over pair production for the large quark masses [16], it is model dependent, and it could be suppressed if the mixing with SM quarks is small.

There are searches for pair production and single production of new heavy quarks at the LHC. The ATLAS and CMS collaborations focused on decay modes of new heavy quarks into a massive vector boson and a third-generation quark assuming a 100% branching ratio, based on $L_{\mathrm{int}} \approx 20\,\mathrm{fb}^{-1}$ of pp collision data at $\sqrt{s} = 8$ TeV, and set lower mass limit for up-type new heavy quark as $m_{t'} > 700$ GeV [17] and $m_{t'} > 735$ GeV [18].

In this work, we investigate the single production of new heavy quarks via FCNC interactions through Z' boson exchange at the LHC. This paper aims at studying the signal and background in detail within the same MC framework, and the relevant interaction vertices are implemented into the MC software. Analyzing the signal observability (via contour plots) for different mass values of the Z' boson and new heavy quarks as well as the mixing parameter through FCNC interactions are another feature of the work. In Section 2, we calculate the decay widths and branching ratios of Z' boson for the mass range 1500–3000 GeV in the framework of different Z' models. An analysis of the parameter space of mass and coupling strength is given for the single production of new heavy quarks at the LHC in Section 3. We analyzed the signal observability for the $Z'q\bar{q}'$ FCNC interactions. We consider both $t'\bar{t}$ and $\bar{t}'t$ single new heavy quark productions for the purpose of enriching the signal statistics even at the small couplings. For the t' quark decay we consider bW^+ mode within the interested parameter space. The analysis for the signal significance is given in Section 4 and the work ends up with the conclusions as given in Section 5.

2. FCNC Interactions

In the gauge eigenstate basis, we can write the additional neutral current Lagrangian related to the $U(1)'$ gauge symmetry by following the formalism given in [11, 19, 20]

$$\mathscr{L}' = -g' \sum_{f,f'} \overline{f} \gamma^{\mu} \left[\epsilon_L \left(ff' \right) P_L + \epsilon_R \left(ff' \right) P_R \right] f' Z'_{\mu}, \quad (1)$$

where $\epsilon_{L,R}(ff')$ are the chiral couplings of Z' boson with fermions f and f'. g' is the gauge coupling of $U(1)'$ and $P_{R,L} = (1 \pm \gamma^5)/2$. Here, it is presumed that there is no mixing between the Z and Z' bosons as favored by the precision data. If the chiral couplings are nondiagonal matrices flavor changing neutral currents (FCNCs) will arise. FCNC couplings come out by fermion mixing if the Z' couplings are diagonal but nonuniversal. Here, we assume that all FCNCs are in the left-hand sector and only for up-type quarks, and the specific form of the mixing matrix is used. Our assumptions can be considered within a model framework (e.g., a particular class of string models [21, 22]) and an ad hoc illustration of a constrained formalism. In the interaction basis the FCNC for the up-type quarks can be given by

$$\mathscr{J}^{u}_{\mathrm{FCNC}} = \left(\overline{u},\ \overline{c},\ \overline{t},\ \overline{t}' \right) \gamma_{\mu} \left(\epsilon^{u}_{L} P_L + \epsilon^{u}_{R} P_R \right) \begin{pmatrix} u \\ c \\ t \\ t' \end{pmatrix}, \quad (2)$$

where the chiral couplings can be written as

$$\epsilon^{u}_{L} = C^{u}_{L} \begin{pmatrix} 1 & 0 & 0 & 0 \\ 0 & 1 & 0 & 0 \\ 0 & 0 & 1 & 0 \\ 0 & 0 & 0 & x \end{pmatrix},$$
$$\epsilon^{u}_{R} = C^{u}_{R} \begin{pmatrix} 1 & 0 & 0 & 0 \\ 0 & 1 & 0 & 0 \\ 0 & 0 & 1 & 0 \\ 0 & 0 & 0 & 1 \end{pmatrix}. \quad (3)$$

The effects of these FCNCs may always arise in the sectors, both up-type and down-type ones after diagonalizing their mass matrices. For simplicity, we suppose that the neutral current couplings to Z' for the right-handed up-sector and

down-sector are family universal and flavor diagonal in the interaction basis. In this case, unitary rotations ($V_{L,R}^{f}$) can maintain the right-handed couplings flavor diagonal, and left-handed sector becomes nondiagonal. The chiral couplings of Z' in the fermion mass eigenstate basis are given by

$$B_L^{ff'} \equiv V_L^f \epsilon_L^u \left(ff'\right) V_L^{f^\dagger},$$
$$B_R^{ff'} \equiv V_R^f \epsilon_R^u \left(ff'\right) V_R^{f^\dagger}. \tag{4}$$

Here, the matrix can be written as $V' = V_L^{u\dagger} V_L^d$; due to our supposition that the down-sector has no mixing it becomes $V' = V_L^{u\dagger}$. The flavor mixing in the left-handed quark fields is simply relevant to this V'. One can find the couplings $B_L^u \equiv V_{uL}^\dagger \epsilon_L^u V_{uL} = V' \epsilon_L^u V'^\dagger$ with the parametrization $|V_{iQ}| = |A_{iQ}|\lambda^{4-i}$ (where the generation index i runs from 1 to 3) for the matrix by assuming the up-sector diagonalization and using unitarity of the CKM matrix.

The FCNC effects from the Z' exchange have been studied for the down-type sector and implications in flavor physics through B-meson decays [23–28] and B-meson mixing [20, 29–33]. These effects have also been studied for up-type quark sector in top quark production [11, 34–38]. The parameters for different Z' models are listed in Table 1. In numerical calculations, the coupling is taken as $g' \simeq 0.40$ for the models.

In our model, the chiral couplings can be written as

$$B_L^u \approx C_L^u \begin{pmatrix} 1+(x-1)\left|A_{14}\right|^2\lambda^6 & (x-1)\,A_{14}A_{24}^*\lambda^5 & (x-1)\,A_{14}A_{34}^*\lambda^4 & (x-1)\,A_{14}A_{44}^*\lambda^3 \\ (x-1)\,A_{24}A_{14}^*\lambda^5 & 1+(x-1)\left|A_{24}\right|^2\lambda^4 & (x-1)\,A_{24}A_{34}^*\lambda^3 & (x-1)\,A_{24}A_{44}^*\lambda^2 \\ (x-1)\,A_{34}A_{14}^*\lambda^4 & (x-1)\,A_{34}A_{24}^*\lambda^3 & 1+(x-1)\left|A_{34}\right|^2\lambda^2 & (x-1)\,A_{34}A_{44}^*\lambda^1 \\ (x-1)\,A_{44}A_{14}^*\lambda^3 & (x-1)\,A_{44}A_{24}^*\lambda^2 & (x-1)\,A_{44}A_{34}^*\lambda^1 & 1+(x-1)\left|A_{44}\right|^2 \end{pmatrix}. \tag{5}$$

The values of the matrix elements $|A_{14}| = 3.2$, $|A_{24}| = 2.0$, and $|A_{34}| = 3.0$ are used as given in [39] by taking into account $\lambda = 0.22$ and $|A_{44}| \simeq 1$. For a comparison, we also calculate the cross sections using the scenario of equal parameters $|A_{i4}| = 2.0$ (where i runs from 1 to 3).

For the FCNC constraints from $D^0 - \overline{D}^0$ mixing with parameter $x_D \simeq 6 \times 10^{-3}$, we follow the calculations performed in [11] and find that the contribution from Z' boson (through FCNC effects) can be obtained as $x_D^{Z'} \simeq 2 \times 10^4 (C_L^{uc})^2$, where $C_L^{uc} = C_L^u(x-1)|A_{14}||A_{24}|\lambda^5$. With the given parametrizations above, this is translated into the result that as long as the combination $|C_L^u(x-1)|$ is less than about 0.3 the experimental bounds can be well satisfied in different Z' models that we have studied in this work.

3. Single Production of New Heavy Quarks

For numerical calculations we have implemented the $Z'qq'$ interaction vertices into the CalcHEP program package [40]. The decay widths of Z' boson for different mass values within different Z' models are tabulated in Table 2. In consideration of the parameter $x = 1$, the couplings to both the left-handed and right-handed ones become universal and family diagonal. In this case, it is hard to see the FCNC effects on the decay widths and cross sections. For the FCNC effects on the decay width, we take the parameter $x = 0.1$ as shown in Figure 1. All these scenarios of Z' models predict a narrow decay width ranging from 0.6% to 3% for $\Gamma_{Z'}/M_{Z'}$ depending on the mass of Z' boson foreseen by different models, for the considered set of parameters. The effect of the FCNC reduces the decay width in the relevant mass range. The decay widths are compared with similar results from [11, 12] for $x = 0.1$ to prove the implementation. Unless otherwise stated throughout this work, we use the FCNC mixing parameter $x = 0.1$ and the mass value of t' quark $m_{t'} = 700$ GeV and the mass value of new heavy charged lepton $m_{l'} = 200$ GeV and new heavy neutrino $m_{\nu'} = 100$ GeV. The branching ratios of Z' boson decays depending on Z' boson mass predicted by different Z' models are given in Figures 2–9; specifically they are given in Figures 2, 4, and 6 for the diagonal couplings to quarks and leptons, while they are given in Figures 3, 5, and 7 for the FCNC couplings to different flavors of up-sector quarks within the Z'_η, Z'_χ, and Z'_ψ models, respectively. In Figures 8 and 9, the branchings for leptophobic Z'_{LP} boson decays to pair of quarks with diagonal couplings and FCNC couplings are presented depending on Z' boson mass.

The cross sections obtained by using parton distribution function library CTEQ6L [41] for the process $pp \to (t'\overline{t} + \overline{t'}t) + X$ depending on the Z' boson mass at the LHC ($\sqrt{s}$ =13 TeV) are given in Figures 10 and 11. Here, the Z' boson contributes through the s- and t-channel diagrams, and the cross sections of associated production of single top quarks and single new heavy quarks ($t'\overline{t}$ and $\overline{t'}t$) in the final state are summed. For this process the cross section at $\sqrt{s} =$ 13 TeV is almost 8 times as large as the case at $\sqrt{s} = 8$ TeV.

We plot the p_T distributions of the b-quark in the signal process with $M_{Z'} = 1500$ GeV for the parameter $x = 0.1$ at the pp center of mass energy of 13 TeV as shown in Figure 12. A high p_T cut decreases the background importantly without affecting much the signal cross section in the related Z' mass range. The rapidity distribution of the bottom quarks (b and $\overline{b}$) from the signal are shown in Figure 13 at the collision energy of 13 TeV. In order to enhance the statistics we sum up the b and $\overline{b}$ distributions. There is a bump in the b-quark

Table 1: The chiral couplings of Z' boson with quarks and leptons predicted by different models.

	Z'_χ	Z'_ψ	Z'_η	Z'_{LP}
C_L^u	$-1/2\sqrt{10}$	$1/\sqrt{24}$	$-1/\sqrt{15}$	1/9
C_R^u	$1/2\sqrt{10}$	$-1/\sqrt{24}$	$1/\sqrt{15}$	−8/9
C_L^d	$-1/2\sqrt{10}$	$1/\sqrt{24}$	$-1/\sqrt{15}$	1/9
C_R^d	$-3/2\sqrt{10}$	$-1/\sqrt{24}$	$-1/2\sqrt{15}$	1/9
C_L^e	$3/2\sqrt{10}$	$1/\sqrt{24}$	$1/2\sqrt{15}$	0
C_R^e	$1/2\sqrt{10}$	$-1/\sqrt{24}$	$1/\sqrt{15}$	0
C_L^ν	$3/2\sqrt{10}$	$1/\sqrt{24}$	$1/2\sqrt{15}$	0

Table 2: The total decay widths of Z' boson for different mass values in various models with the FCNC parameter $x = 0.1$. We use the value of masses of new heavy quarks $m_{Q'} = 700$ GeV and the masses of new heavy leptons $m_{l'} = 200$ GeV and $m_{\nu'} = 100$ GeV.

$M_{Z'}$ (GeV)	$\Gamma(Z'_\chi)$ (GeV)	$\Gamma(Z'_\psi)$ (GeV)	$\Gamma(Z'_\eta)$ (GeV)	$\Gamma(Z'_{\mathrm{LP}})$ (GeV)
1400	17.25	7.73	9.21	28.85
1600	21.75	9.20	11.61	37.44
1800	25.11	10.66	13.46	43.99
2000	28.30	12.11	15.22	50.25
2200	31.41	13.55	16.95	56.36
2400	34.48	14.98	18.65	62.36
2600	37.53	16.40	20.33	68.30
2800	40.55	17.82	22.01	74.18
3000	43.56	19.23	23.67	80.02

rapidity distribution $\eta^b \simeq 0$ with the extending tails to $|\eta^b| \simeq 2.5$. For the analysis, the suitable cuts are $p_T^{b,\bar{b}} > 100$ GeV, $|\eta^{b,\bar{b}}| \leq 2.0$, and $m_{Wb} > 400$ GeV. The cut m_{Wb} is also useful well above the top quark mass. We also apply invariant mass cut (for Wbt system) $M_{Z'} - 4\Gamma_{Z'} < m_{Wbt} < M_{Z'} + 4\Gamma$ to make analysis with the signal and background.

The signal cross sections (σ_S) in the invariant mass interval of $M_{Z'} - 4\Gamma_{Z'} < m_{Wbt} < M_{Z'} + 4\Gamma$, for the process $pp \to (W^+b\bar{t} + W^-\bar{b}t) + X$, are given in Tables 3, 4, 5, and 6 for different values of FCNC parameter x (ranging from 0.01 to 0.5) within the Z'_η (Z'_χ) model, where new heavy quark masses are taken 600 GeV, 700 GeV, and 800 GeV. For the Z'_ψ (Z'_{LP}) model and the FCNC parameter for 0.01, 0.05, 0.1, and 0.5, the cross sections (σ_S) are presented in Tables 7, 8, 9, and 10, respectively. The cross sections for the corresponding background are given in Table 11 for the chosen invariant mass interval.

Figures 14, 15, 16, and 17 show the invariant mass distribution of the Wbt system for the signal (with $x = 0.1$ and $m_{t'} = 700$ sGeV) of different Z' models and background at the LHC with $\sqrt{s} = 13$ TeV.

4. Analysis

For the analysis, two types of backgrounds are considered. One has the same final state (Wbt) as expected for the signal processes and the other (pair productions of top quarks are both related to b-jets) is the irreducible background and contributes to similar final state. The ratio of the cross sections for pair production of top quarks at the $\sqrt{s} = 13$ TeV and $\sqrt{s} = 8$ TeV is about 3.5. The ratio of the cross sections for

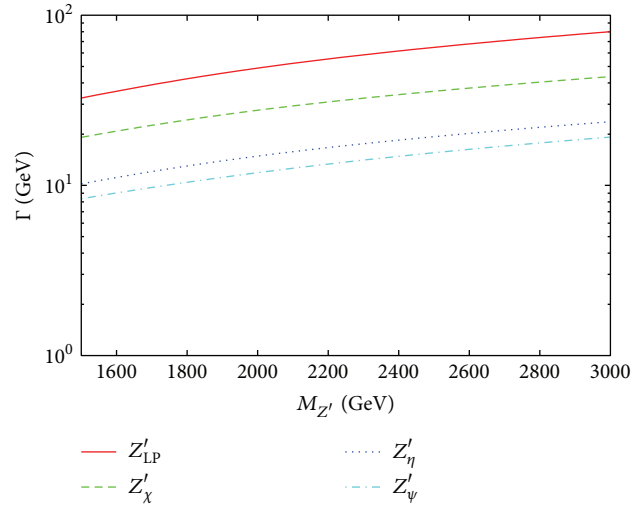

Figure 1: The decay widths of Z' boson depending on its mass for different Z' models with the FCNC parameter $x = 0.1$. Here, we use the mass value of new heavy quarks as 700 GeV and the mass value of new heavy charged lepton and neutrino as 200 GeV and 100 GeV, respectively.

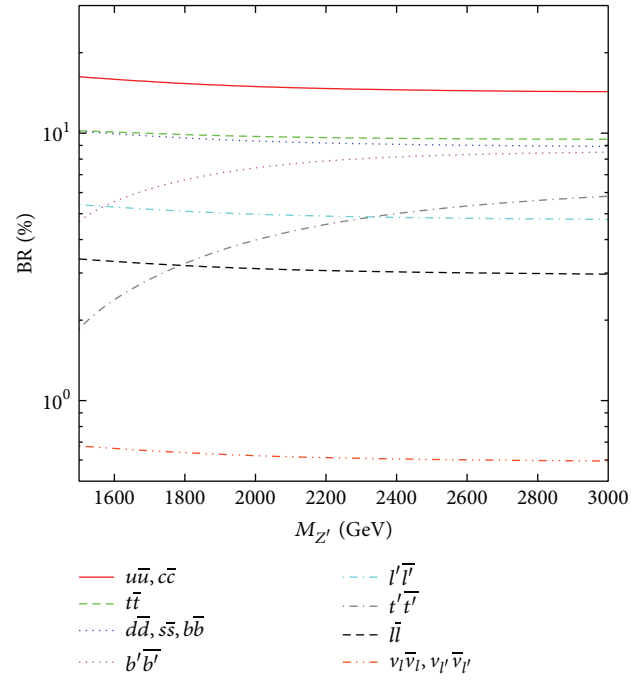

Figure 2: Branching ratios (%) depending on the mass of Z' boson for diagonal couplings to quarks and leptons within the Z'_η model. The new heavy quark masses are taken to be 700 GeV, and new heavy charged lepton mass is 200 GeV and new heavy neutrino mass is 100 GeV.

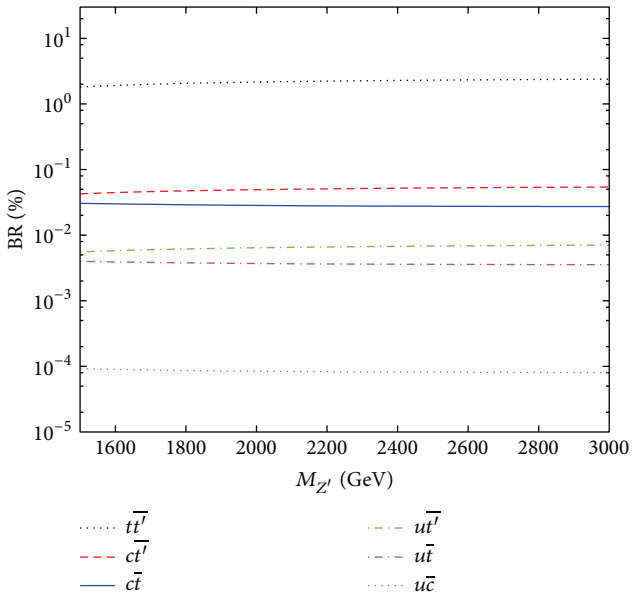

FIGURE 3: Branching ratios (%) depending on the mass of the Z' boson for FCNC couplings to different flavors of up-sector quarks within the Z'_η model. Here the mass of t' quark is 700 GeV and the FCNC parameter $x = 0.1$.

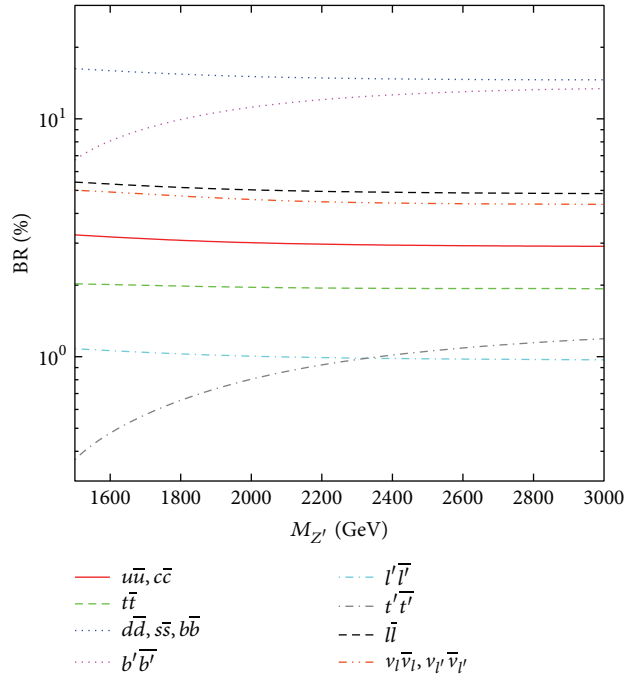

FIGURE 4: Branching ratios (%) depending on the mass of Z' boson for diagonal couplings to quarks and leptons within the Z'_χ model. The new heavy quark masses are taken to be 700 GeV, and new heavy charged lepton mass is 200 GeV and new heavy neutrino mass is 100 GeV.

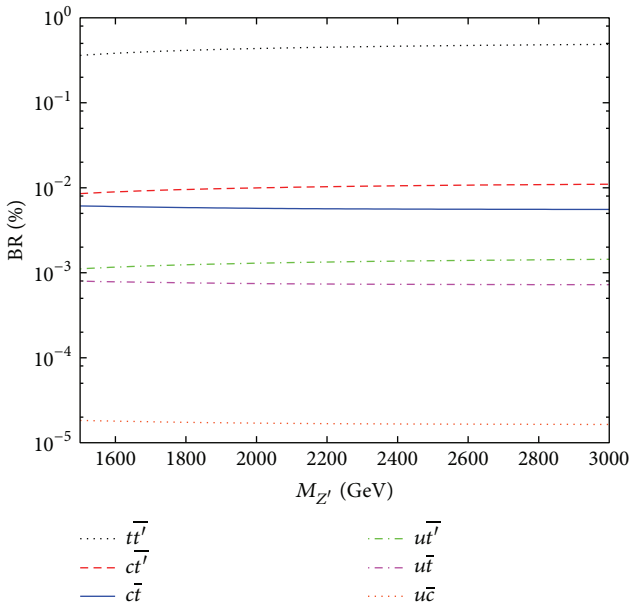

FIGURE 5: Branching ratios (%) depending on the mass of the Z' boson for FCNC couplings to different flavors of up-sector quarks within the Z'_χ model. Here the mass of t' quark is 700 GeV and the FCNC parameter $x = 0.1$.

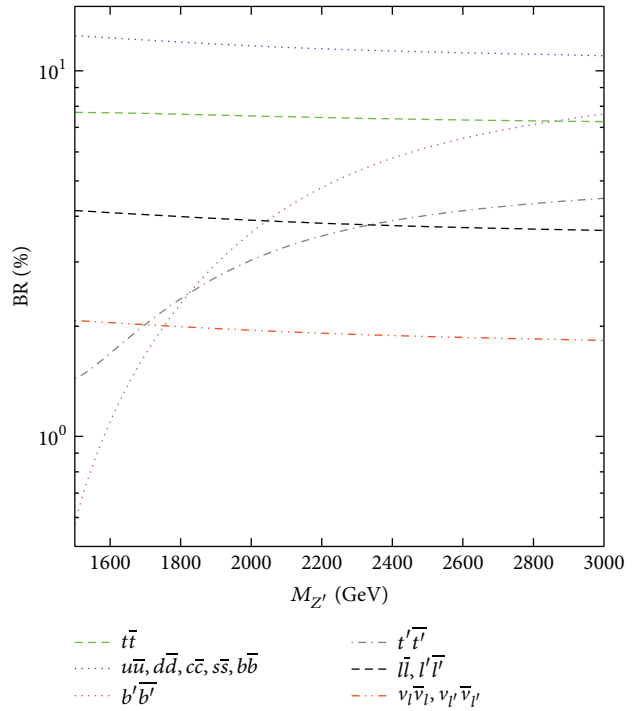

FIGURE 6: Branching ratios (%) depending on the mass of Z' boson for diagonal couplings to quarks and leptons within the Z'_ψ model. The new heavy quark masses are taken to be 700 GeV, and new heavy charged lepton mass is 200 GeV and new heavy neutrino mass is 100 GeV.

process $pp \to (t'\bar{t} + \bar{t}'t) + X$ is found to be about 8 for considered Z' models. It is expected that an improvement in the statistical significance (for the center of mass energy $\sqrt{s} =$ 13 TeV when compared to the case of $\sqrt{s} = 8$ TeV) will be obtained. For the analysis, a high transverse momentum (p_T)

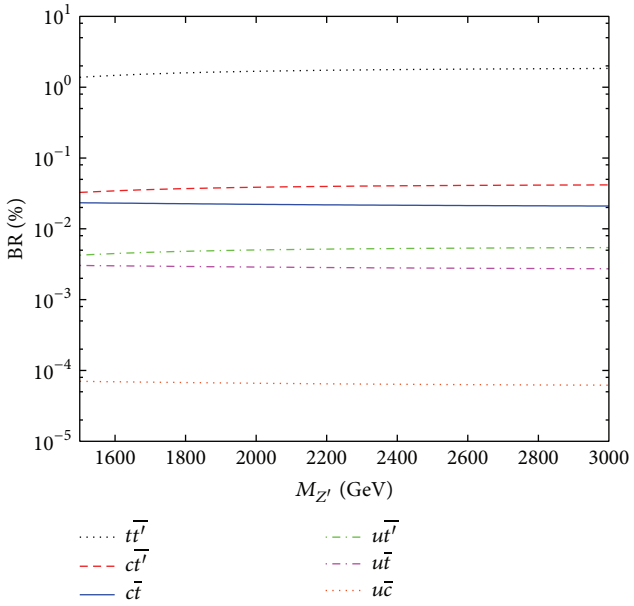

FIGURE 7: Branching ratios (%) depending on the mass of the Z' boson for FCNC couplings to different flavors of up-sector quarks within the Z'_{ψ} model. Here the mass of t' quark is 700 GeV and the FCNC parameter $x = 0.1$.

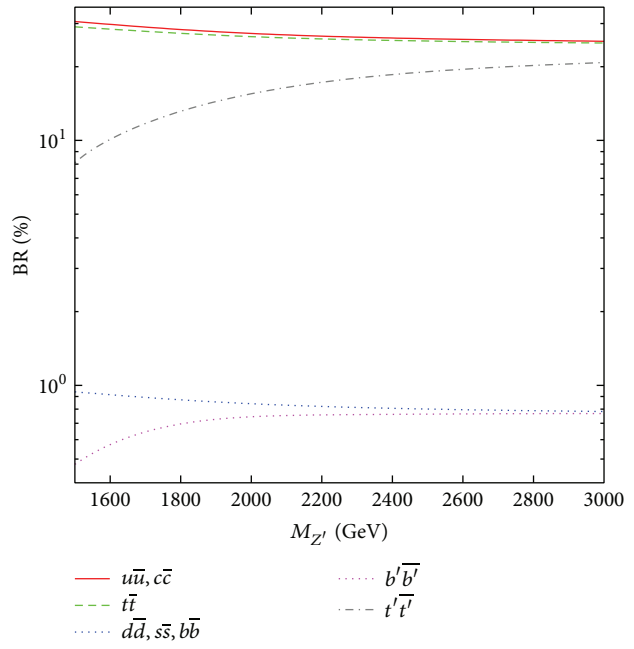

FIGURE 8: Branching ratios (%) depending on the mass of Z' boson for diagonal couplings to quarks within the Z'_{LP} model. The new heavy quark masses are taken to be 700 GeV.

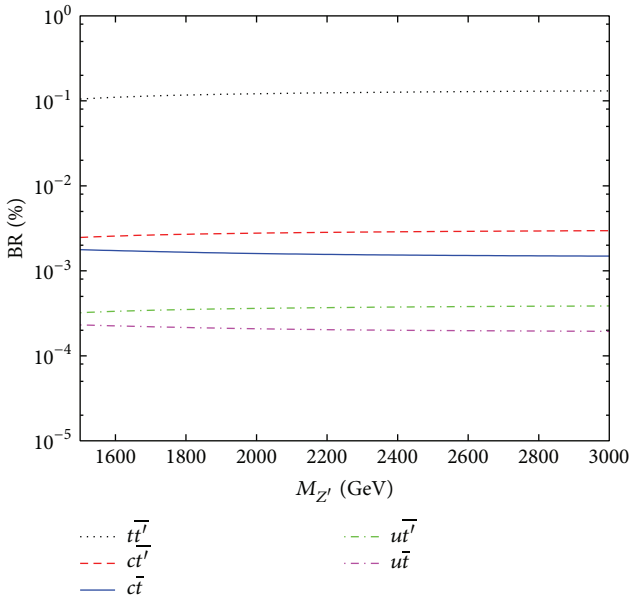

FIGURE 9: Branching ratios (%) depending on the mass of the Z' boson for FCNC couplings to different flavors of up-sector quarks within the Z'_{LP} model. Here the mass of t' quark is 700 GeV and the FCNC parameter $x = 0.1$.

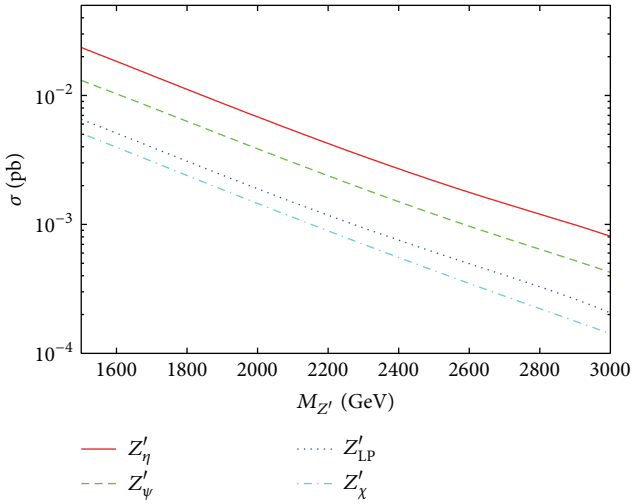

FIGURE 10: The cross sections for $pp \to (t'\bar{t} + \bar{t}'t) + X$ versus the Z' boson mass at the LHC with $\sqrt{s} = 13$ TeV. The lines are for different Z' models as explained in the text, where the parameters $|A_{14}| = 3.2$, $|A_{24}| = 2.0$, and $|A_{34}| = 3.0$ are used. The mass value of t' quark is used as $m_{t'} = 700$ GeV and the FCNC parameter is used as $x = 0.1$.

cut for the b-jets and the other jets can be applied. The results, employing the variable p_T cuts ($p_T > 100$ GeV) for different Z' mass values and the rapidity cuts ($|\eta| < 2$) for the central detector coverage, are given in Tables 12, 13, 14, and 15, where the numbers of signal (S) and background (B) events are calculated by taking into consideration integrated luminosity of $L_{\mathrm{int}} = 10^5$ pb^{-1} per year. For the FCNC coupling parameter $x = 0.1$, the LHC is able to measure the Z' mass up to about 3000 GeV with the associated productions of the new heavy quark t' and top quark. The statistical significance (SS) values for the final state are given in Tables 12–15 for different Z' boson masses.

In the analysis, we reconstruct the invariant mass of Wbt system around the Z' boson mass shown in Figures 14, 15, 16, and 17. We assume top quark decay in the form of $t(\bar{t}) \to$

Table 3: The total cross section for the signal (σ_S) depending on the Z' boson mass. These values are calculated for the process $pp \to (W^+b\bar{t} + W^-\bar{b}t) + X$ at the LHC with $\sqrt{s} = 13$ TeV. The results are obtained for the Z'_η model (the Z'_χ model) with the FCNC parameter $x = 0.01$.

$M_{Z'}$ (GeV)	σ_S (pb)		
	$m_{t'} = 600$ GeV	$m_{t'} = 700$ GeV	$m_{t'} = 800$ GeV
1500	2.44×10^{-2} (5.51×10^{-3})	2.23×10^{-2} (4.98×10^{-3})	1.98×10^{-2} (4.41×10^{-3})
2000	7.31×10^{-3} (1.60×10^{-3})	6.95×10^{-3} (1.51×10^{-3})	6.49×10^{-3} (1.41×10^{-3})
2500	2.40×10^{-3} (5.05×10^{-4})	2.33×10^{-3} (4.90×10^{-4})	2.24×10^{-3} (4.70×10^{-4})
3000	1.01×10^{-3} (1.74×10^{-4})	9.93×10^{-4} (1.71×10^{-4})	9.71×10^{-4} (1.67×10^{-4})

Table 4: The same as Table 3, but for $x = 0.05$.

$M_{Z'}$ (GeV)	σ_S (pb)		
	$m_{t'} = 600$ GeV	$m_{t'} = 700$ GeV	$m_{t'} = 800$ GeV
1500	2.26×10^{-2} (5.06×10^{-3})	2.06×10^{-2} (4.59×10^{-3})	1.82×10^{-2} (4.07×10^{-3})
2000	6.75×10^{-3} (1.47×10^{-3})	6.44×10^{-3} (1.40×10^{-3})	6.00×10^{-3} (1.29×10^{-3})
2500	2.22×10^{-3} (4.65×10^{-4})	2.16×10^{-3} (4.51×10^{-4})	2.07×10^{-3} (4.32×10^{-4})
3000	9.28×10^{-4} (1.60×10^{-4})	9.17×10^{-4} (1.58×10^{-4})	8.96×10^{-4} (1.54×10^{-4})

Table 5: The same as Table 3, but for $x = 0.1$.

$M_{Z'}$ (GeV)	σ_S (pb)		
	$m_{t'} = 600$ GeV	$m_{t'} = 700$ GeV	$m_{t'} = 800$ GeV
1500	2.04×10^{-2} (4.55×10^{-3})	1.86×10^{-2} (4.12×10^{-3})	1.64×10^{-2} (3.66×10^{-3})
2000	6.10×10^{-3} (1.32×10^{-3})	5.81×10^{-3} (1.25×10^{-3})	5.42×10^{-3} (1.16×10^{-3})
2500	2.00×10^{-3} (4.19×10^{-4})	1.95×10^{-3} (4.05×10^{-4})	1.87×10^{-3} (3.89×10^{-4})
3000	8.34×10^{-4} (1.44×10^{-4})	8.23×10^{-4} (1.42×10^{-4})	8.04×10^{-4} (1.38×10^{-4})

Table 6: The same as Table 3, but for $x = 0.5$.

$M_{Z'}$ (GeV)	σ_S (pb)		
	$m_{t'} = 600$ GeV	$m_{t'} = 700$ GeV	$m_{t'} = 800$ GeV
1500	6.45×10^{-3} (1.41×10^{-3})	5.85×10^{-3} (1.28×10^{-3})	5.09×10^{-3} (1.13×10^{-3})
2000	1.91×10^{-3} (4.09×10^{-4})	1.82×10^{-3} (3.89×10^{-4})	1.71×10^{-3} (3.61×10^{-4})
2500	6.22×10^{-4} (1.30×10^{-4})	6.09×10^{-4} (1.26×10^{-4})	5.87×10^{-4} (1.20×10^{-4})
3000	2.55×10^{-4} (4.43×10^{-5})	2.51×10^{-4} (4.36×10^{-5})	2.47×10^{-4} (4.26×10^{-5})

Table 7: The total cross section values for the signal (σ_S) are calculated for the process $pp \to (W^+b\bar{t}+W^-\bar{b}t)+X$ at the LHC with $\sqrt{s} = 13$ TeV. The results are obtained for the Z'_ψ model (the Z'_{LP} model) and the FCNC parameter $x = 0.01$.

$M_{Z'}$ (GeV)	σ_S (pb)		
	$m_{t'} = 600$ GeV	$m_{t'} = 700$ GeV	$m_{t'} = 800$ GeV
1500	1.42×10^{-2} (6.22×10^{-3})	1.28×10^{-2} (5.77×10^{-3})	1.08×10^{-2} (5.20×10^{-3})
2000	4.13×10^{-3} (1.84×10^{-3})	3.97×10^{-3} (1.77×10^{-3})	3.72×10^{-3} (1.67×10^{-3})
2500	1.33×10^{-3} (6.13×10^{-4})	1.30×10^{-3} (6.01×10^{-4})	1.26×10^{-3} (5.82×10^{-4})
3000	5.24×10^{-4} (3.00×10^{-4})	5.20×10^{-4} (3.00×10^{-4})	5.13×10^{-4} (2.95×10^{-4})

Table 8: The same as Table 7, but for $x = 0.05$.

$M_{Z'}$ (GeV)	σ_S (pb)		
	$m_{t'} = 600$ GeV	$m_{t'} = 700$ GeV	$m_{t'} = 800$ GeV
1500	1.31×10^{-2} (5.72×10^{-3})	1.18×10^{-2} (5.33×10^{-3})	9.90×10^{-3} (4.79×10^{-3})
2000	3.82×10^{-3} (1.70×10^{-3})	3.67×10^{-3} (1.64×10^{-3})	3.43×10^{-3} (1.55×10^{-3})
2500	1.23×10^{-3} (5.64×10^{-4})	1.20×10^{-3} (5.54×10^{-4})	1.17×10^{-3} (5.35×10^{-4})
3000	4.84×10^{-4} (1.77×10^{-4})	5.21×10^{-4} (2.76×10^{-4})	4.72×10^{-4} (2.72×10^{-4})

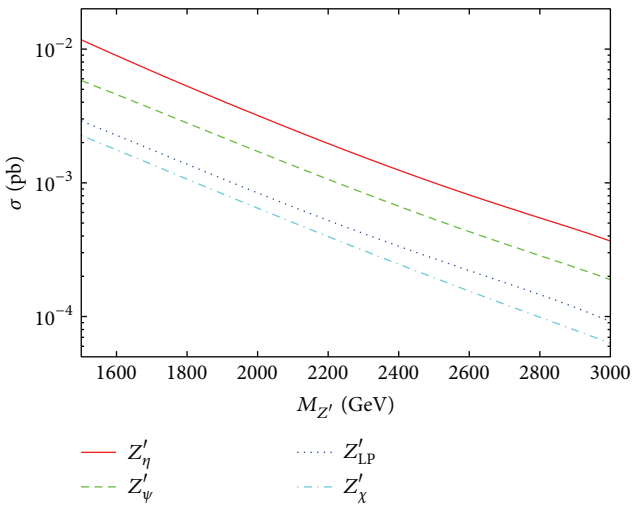

FIGURE 11: The cross sections for $pp \to (t'\bar{t} + \bar{t}'t) + X$ versus the Z' boson mass at the LHC with $\sqrt{s} = 13$ TeV. The lines are for the four Z' models as explained in the text and the values of parameters $|A_{i4}| = 2$ (where i runs from 1 to 3) are used. The mass value of t' quark is used as $m_{t'} = 700$ GeV and the FCNC parameter is used as $x = 0.1$.

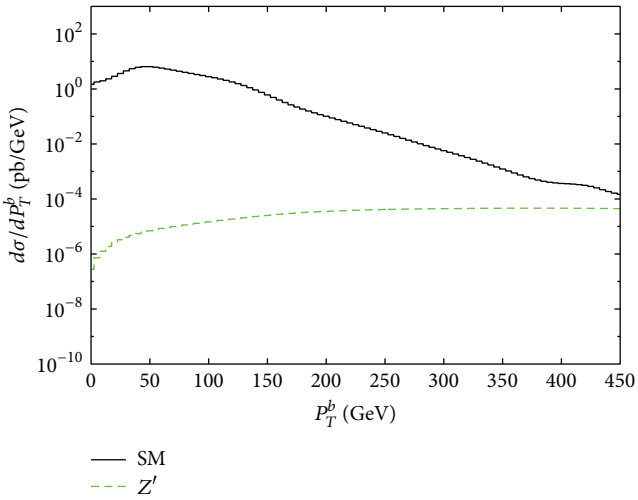

FIGURE 12: The transverse momentum (p_T) distribution of the bottom quarks (b and $\bar{b}$) for the signal and background processes $pp \to (W^+b\bar{t} + W^-\bar{b}t) + X$ at the LHC with $\sqrt{s} = 13$ TeV for the parameters explained in the text. These results are obtained for the Z'_η model.

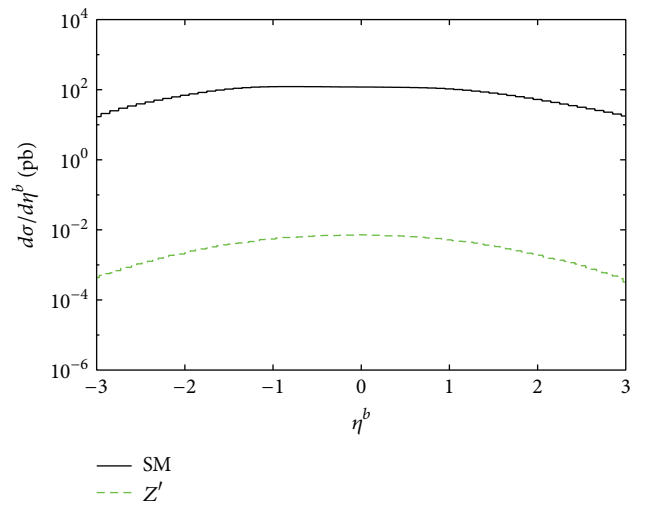

FIGURE 13: The pseudorapidity distribution of the bottom quarks (b and $\bar{b}$) for the signal (Z') and background processes (SM) $pp \to (W^+b\bar{t} + W^-\bar{b}t) + X$ at the LHC with $\sqrt{s} = 13$ TeV for the parameters explained in the text. The results are obtained for the Z'_η model.

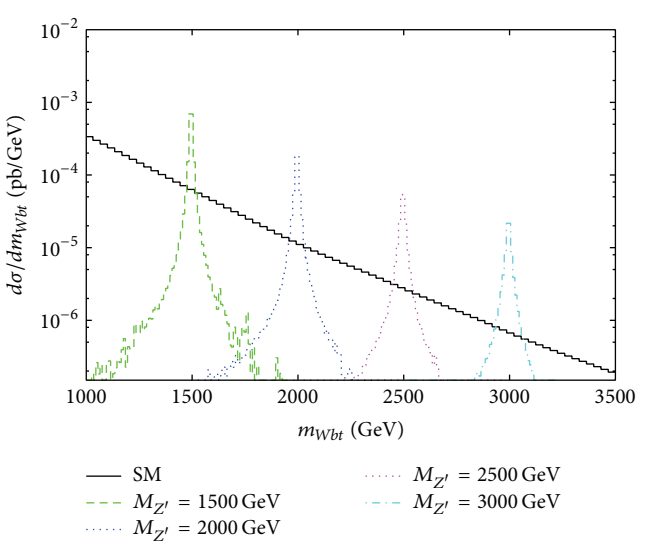

FIGURE 14: The invariant mass distribution of the $(W^+b\bar{t} + \overline{W^-}\bar{b}t)$ system for the SM and Z'_η model with different mass values of Z' boson at the LHC with $\sqrt{s} = 13$ TeV. The results are obtained for $x = 0.1$ and $m_{t'} = 700$ GeV.

$W^+b(W^-\bar{b})$, where the W boson can decay leptonically or hadronically. In the final state $W^+W^-b\bar{b}$, we assume the b-tagging efficiency as 50% for each of the b-quarks. We take into account the channel in which one of the W bosons decays leptonically, while the other decays hadronically. We calculate the cross section of the background in the mass bin widths for each $M_{Z'}$ value; as an example of the Z'_η model, for $M_{Z'} = 1500$ GeV we take the invariant mass interval $\Delta m_{Wbt} \simeq 40$ GeV, and we find the background cross section $\sigma_B = 6.60 \times 10^{-3}$ pb for process $pp \to (W^-\bar{b}t + W^+b\bar{t}) + X$.

We plot the observability contours in the plane of model parameters ($x - M_{Z'}$), for different Z' models as shown in Figure 18 at the LHC with $\sqrt{s} = 13$ TeV and $L_{\text{int}} = 100\,\text{fb}^{-1}$. The curves with labels Z'_{LP}, Z'_χ, Z'_ψ, and Z'_η show the accessible regions (below the curves) of the model parameters at the LHC. For the Z'_η model, the FCNC parameter bounds from $x = 0.6$–0.4 can be searched for the mass range of $M_{Z'} = 1500$–3000 GeV.

Table 9: The same as Table 7, but for $x = 0.1$.

$M_{Z'}$ (GeV)	σ_S (pb)		
	$m_{t'} = 600$ GeV	$m_{t'} = 700$ GeV	$m_{t'} = 800$ GeV
1500	1.18×10^{-2} (5.17×10^{-3})	1.06×10^{-2} (4.78×10^{-3})	8.93×10^{-3} (4.30×10^{-3})
2000	3.43×10^{-3} (1.53×10^{-3})	3.30×10^{-3} (1.47×10^{-3})	3.10×10^{-3} (1.39×10^{-3})
2500	1.11×10^{-3} (5.06×10^{-4})	1.09×10^{-3} (4.97×10^{-4})	1.05×10^{-3} (4.82×10^{-4})
3000	4.33×10^{-4} (2.49×10^{-4})	4.31×10^{-4} (2.48×10^{-4})	4.24×10^{-4} (2.44×10^{-4})

Table 10: The same as Table 7, but for $x = 0.5$.

$M_{Z'}$ (GeV)	σ_S (pb)		
	$m_{t'} = 600$ GeV	$m_{t'} = 700$ GeV	$m_{t'} = 800$ GeV
1500	3.72×10^{-3} (1.60×10^{-3})	3.34×10^{-3} (1.49×10^{-3})	2.78×10^{-3} (1.33×10^{-3})
2000	1.08×10^{-3} (4.74×10^{-4})	1.04×10^{-3} (4.57×10^{-4})	9.72×10^{-4} (4.31×10^{-4})
2500	3.44×10^{-4} (1.57×10^{-4})	3.39×10^{-4} (1.54×10^{-4})	3.29×10^{-4} (1.49×10^{-4})
3000	1.33×10^{-4} (7.69×10^{-5})	1.32×10^{-4} (7.66×10^{-5})	1.30×10^{-4} (7.57×10^{-5})

Table 11: The cross section for the background (σ_B) depending on the values of invariant mass interval. The values are calculated for the process $pp \to (W^+b\bar{t} + W^-\bar{b}t)X$ at the LHC with $\sqrt{s} = 13$ TeV. The results are given in the invariant mass within $M_{Z'} - 4\Gamma_{Z'} < m_{Wbt} < M_{Z'} + 4\Gamma_{Z'}$ for different Z' decay widths corresponding to the parameters explained in the text.

m_{Wbt} (GeV)	σ_B (pb)			
	(for $\Gamma_{Z'_\eta}$ width)	(for $\Gamma_{Z'_\chi}$ width)	(for $\Gamma_{Z'_\psi}$ width)	(for $\Gamma_{Z'_{LP}}$ width)
$1500 \pm 4\Gamma_{Z'}$	6.60×10^{-3}	1.34×10^{-2}	5.63×10^{-3}	2.33×10^{-2}
$2000 \pm 4\Gamma_{Z'}$	1.87×10^{-3}	3.54×10^{-3}	1.50×10^{-3}	6.72×10^{-3}
$2500 \pm 4\Gamma_{Z'}$	5.26×10^{-4}	1.02×10^{-3}	4.34×10^{-4}	1.97×10^{-3}
$3000 \pm 4\Gamma_{Z'}$	1.67×10^{-4}	3.09×10^{-4}	1.33×10^{-4}	6.23×10^{-4}

Table 12: The number of signal and background events for the final state $l^\pm + 2b_{\text{jet}} + 2\text{jet} + \text{MET}$ at the center of mass energy $\sqrt{s} = 13$ TeV and integrated luminosity $L_{\text{int}} = 10^5$ pb^{-1}. The numbers in the parentheses denote the signal significances (SS). These results are achieved for the Z'_η model and parameter $x = 0.1$.

$M_{Z'_\eta}$ (GeV)	Signal – $(t'\bar{t} + \bar{t'}t) \to 2 \times (l^\pm + 2b_{\text{jet}} + 2\text{jet} + \text{MET})$			Background – $(W^+b\bar{t} + W^-\bar{b}t)$
	$m_{t'} = 600$ GeV	$m_{t'} = 700$ GeV	$m_{t'} = 800$ GeV	$2 \times (l^\pm + 2b_{\text{jet}} + 2\text{jet} + \text{MET})$
1500	305.0 (30.7)	277.8 (28.0)	245.6 (24.7)	98.6
2000	91.2 (17.3)	68.8 (16.4)	81.0 (15.3)	28.0
2500	30.0 (10.6)	29.2 (10.3)	28.0 (9.9)	7.8
3000	12.4 (7.9)	12.4 (7.8)	12.0 (7.6)	2.6

Table 13: The same as Table 12, but for Z'_χ.

$M_{Z'_\chi}$ (GeV)	Signal – $(t'\bar{t} + \bar{t'}t) \to 2 \times (l^\pm + 2b_{\text{jet}} + 2\text{jet} + \text{MET})$			Background – $(W^+b\bar{t} + W^-\bar{b}t)$
	$m_{t'} = 600$ GeV	$m_{t'} = 700$ GeV	$m_{t'} = 800$ GeV	$2 \times (l^\pm + 2b_{\text{jet}} + 2\text{jet} + \text{MET})$
1500	68.0 (4.8)	61.6 (4.4)	54.8 (4.0)	200.4
2000	19.8 (2.7)	18.8 (2.5)	17.4 (2.4)	53.0
2500	6.2 (1.6)	6.0 (1.6)	5.8 (1.6)	15.2
3000	2.2 (1.4)	2.2 (1.4)	2.0 (1.4)	4.6

Table 14: The same as Table 12, but for Z'_ψ.

$m_{Z'_\psi}$ (GeV)	Signal – $(t'\bar{t} + \bar{t'}t) \to 2 \times (l^\pm + 2b_{\text{jet}} + 2\text{jet} + \text{MET})$			Background $-(W^+b\bar{t} + W^-\bar{b}t)$
	$m_{t'} = 600$ GeV	$m_{t'} = 700$ GeV	$m_{t'} = 800$ GeV	$2 \times (l^\pm + 2b_{\text{jet}} + 2\text{jet} + \text{MET})$
1500	176.5 (19.2)	158.6 (17.3)	133.6 (14.6)	84.2
2000	51.3 (10.8)	49.4 (10.4)	46.4 (9.8)	22.4
2500	16.6 (6.5)	16.3 (6.4)	15.7 (6.2)	6.5
3000	6.5 (4.6)	6.4 (4.5)	6.3 (4.6)	2.0

Table 15: The same as Table 12, but for Z'_{LP}.

$M_{Z'_{\mathrm{LP}}}$ (GeV)	Signal – $(t'\bar{t} + \bar{t}'t) \to 2 \times (l^{\pm} + 2b_{\mathrm{jet}} + 2\mathrm{jet} + \mathrm{MET})$			Background – $(W^+b\bar{t} + W^-\bar{b}t)$
	$m_{t'} = 600$ GeV	$m_{t'} = 700$ GeV	$m_{t'} = 800$ GeV	$2 \times (l^{\pm} + 2b_{\mathrm{jet}} + 2\mathrm{jet} + \mathrm{MET})$
1500	77.3 (4.1)	71.5 (3.8)	64.3 (3.4)	348.5
2000	22.9 (2.3)	22.0 (2.2)	20.8 (2.1)	100.5
2500	7.6 (1.4)	7.4 (1.4)	7.2 (1.3)	29.5
3000	3.7 (1.2)	3.7 (1.2)	3.7 (1.2)	9.3

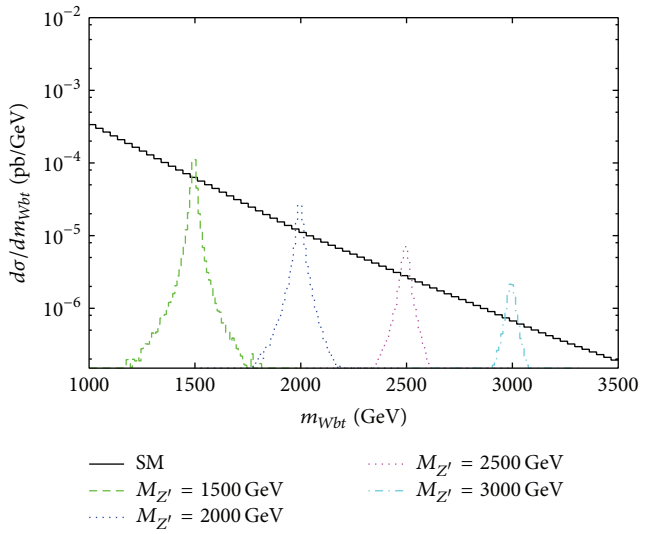

Figure 15: The same as Figure 13, but for Z'_{χ} model.

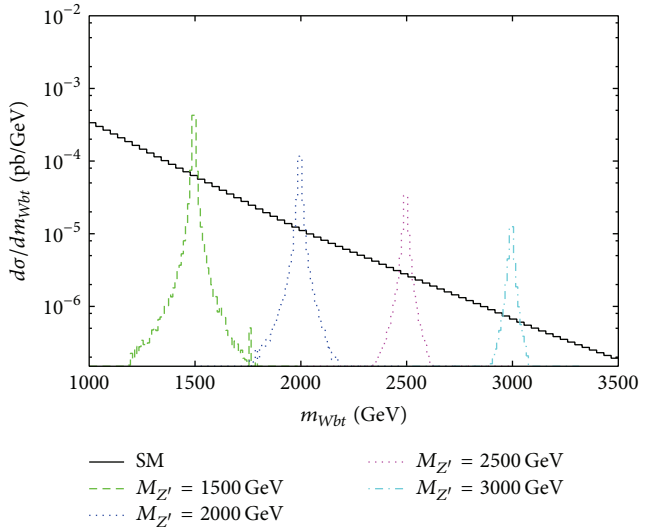

Figure 16: The same as Figure 13, but for Z'_{ψ} model.

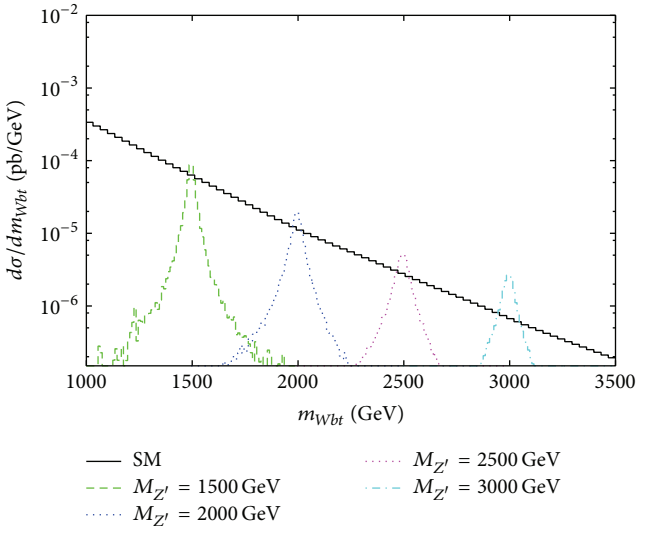

Figure 17: The same as Figure 13, but for Z'_{LP} model.

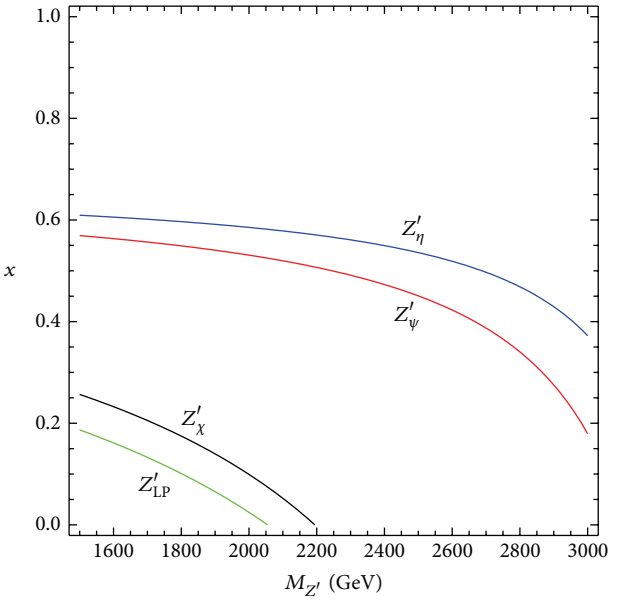

Figure 18: The contour plot for the evidence of Z' boson at the LHC ($\sqrt{s} = 13$ TeV) with $L_{\mathrm{int}} = 100\,\mathrm{fb}^{-1}$. The parameters used in the analysis are explained in the text.

5. Conclusion

We consider the associated productions of new heavy quark t' and top quark (with the subsequent decay channel $t' \to W^+b$) through the Z' exchange diagrams at the LHC. We find the discovery regions of the parameter space for the single productions of new heavy quarks through FCNC interactions with the new Z' boson. In the models considered in this

paper, the single production of new heavy quarks at the LHC can have the contributions from the couplings of $Z'q\bar{q}$ and the FCNC couplings of $Z'q\bar{q}'$ (where $q, q' = u, c, t, t'$). For the FCNC parameter range ($0 < x < 1$ means maximal to minimal FCNC) the LHC can have the potential to produce new heavy quarks which couple to the Z' boson predicted by specific models. For a discussion on the t' decays, in this study we only consider $t' \to bW^+$. It may be possible that $t' \to b'W^*$ which does not have a CKM suppression like $t' \to bW^+$ could compete with this decay mode depending on the mass difference of new t' and b' quarks. However, these channels require a new study which we will tackle as a separate topic of paper at another study.

Competing Interests

The authors declare that they have no competing interests.

Acknowledgments

O. Çakır's work is supported in part by the Turkish Atomic Energy Authority (TAEK) under the project Grant no. 2016TAEK (CERN) A5.H6.F2-14.

References

[1] P. Langacker, "The physics of heavy Z′ gauge bosons," *Reviews of Modern Physics*, vol. 81, no. 3, pp. 1199–1228, 2009.

[2] K. A. Olive, K. Agashe, C. Amsler et al., "Review of particle physics," *Chinese Physics C*, vol. 38, Article ID 090001, 2014.

[3] A. Aad, B. Abbott, J. Abdallah et al., "Search for high-mass dilepton resonances in *pp* collisions at with the $\sqrt{s} = 8$ TeV with the ATLAS detector," *Physical Review D*, vol. 90, no. 5, Article ID 052005, 2014.

[4] A. Aad, T. Abajyan, B. Abbott et al., "Search for high-mass resonances decaying to dilepton final states in *pp* collisions at $\sqrt{s} = 7$ TeV with the ATLAS detector," *Journal of High Energy Physics*, vol. 2012, article 138, 2012.

[5] S. Chatrchyan, V. Khachatryan, A. M. Sirunyan et al., "Search for heavy narrow dilepton resonances in pp collisions at $\sqrt{s} = 7$ Tev and $\sqrt{s} = 8$ Tev," *Physics Letters B*, vol. 720, no. 1–3, pp. 63–82, 2013.

[6] S. Khachatryan, A. M. Sirunyan, A. Tumasyan et al., "Search for physics beyond the standard model in dilepton mass spectra in proton-proton collisions at $\sqrt{s} = 8$ TeV," *Journal of High Energy Physics*, vol. 2015, no. 4, article 025, 2015.

[7] A. Aad, T. Abajyan, B. Abbott et al., "Search for $t\bar{t}$ resonances in the lepton plus jets final state with ATLAS using 4.7 fb^{-1} of *pp* collisions at $\sqrt{s} = 7$ TeV," *Physical Review D*, vol. 88, no. 1, Article ID 012004, 28 pages, 2013.

[8] S. Chatrchyan, V. Khachatryan, A. M. Sirunyan et al., "Searches for new physics using the $t\bar{t}$ invariant mass distribution in *pp* collisions at $\sqrt{s} = 8$ Tev," *Physical Review Letters*, vol. 111, no. 21, Article ID 211804, 16 pages, 2013.

[9] A. Alves, S. Profumo, and F. S. Queiroz, "The dark Z' portal: direct, indirect and collider searches," *Journal of High Energy Physics*, vol. 2014, article 63, 2014.

[10] A. Alves, A. Berlin, S. Profumod, and F. S. Queiroz, "Dirac-fermionic dark matter in $\text{U}(1)_X$ models," *Journal of High Energy Physics*, vol. 2015, article 76, 2015.

[11] A. Arhrib, K. Cheung, C.-W. Chiang, and T.-C. Yuan, "Single top quark production in flavor-changing Z′ models," *Physical Review D*, vol. 73, no. 7, Article ID 075015, 2006.

[12] O. Cakir, I. T. Cakir, A. Senol, and A. T. Tasci, "Search for top quark FCNC couplings in Z′ models at the LHC and CLIC," *The European Physical Journal C*, vol. 70, no. 1-2, pp. 295–303, 2010.

[13] R. Contino, Y. Nomura, and A. Pomarol, "Higgs as a holographic pseudo-Goldstone boson," *Nuclear Physics B*, vol. 671, pp. 148–174, 2003.

[14] J. A. Aguilar-Saavedra, "Mixing with vector-like quarks: constraints and expectations," *EPJ Web of Conferences*, vol. 60, article 16012, 2013.

[15] S. Sultansoy and G. Unel, "The E6 inspired isosinglet quark and the Higgs boson," *Physics Letters, Section B: Nuclear, Elementary Particle and High-Energy Physics*, vol. 669, no. 1, pp. 39–45, 2008.

[16] O. Çakır, İ. T. Çakır, H. D. Yıldız, and R. Mehdiyev, "Single production of fourth-family quarks at the LHC," *The European Physical Journal C*, vol. 56, no. 4, pp. 537–543, 2008.

[17] S. Chatrchyan, V. Khachatryan, A. M. Sirunyan et al., "Inclusive search for a vector-like T quark with charge $\frac{2}{3}$ in pp collisions at $\sqrt{s} = 8$ Tev," *Physics Letters B*, vol. 729, pp. 149–171, 2014.

[18] A. Aad, B. Abbott, J. Abdallah et al., "Search for pair and single production of new heavy quarks that decay to a Z boson and a third-generation quark in pp collisions at $\sqrt{s} = 8$ TeV with the ATLAS detector," *Journal of High Energy Physics*, vol. 2014, article 104, 2014.

[19] P. Langacker and M. Plümacher, "Flavor changing effects in theories with a heavy Z′ boson with family nonuniversal couplings," *Physical Review D*, vol. 62, no. 1, Article ID 013006, 2000.

[20] K. Cheung, C.-W. Chiang, N. G. Deshpande, and J. Jiang, "Constraints on flavor-changing Z' models by B_s mixing, Z' production, and $B_s \to \mu^+\mu^-$," *Physics Letters B*, vol. 652, no. 5-6, pp. 285–291, 2007.

[21] S. Chaudhuri, S.-W. Chung, G. Hockney, and J. Lykken, "String consistency for unified model building," *Nuclear Physics B*, vol. 456, no. 1-2, pp. 89–129, 1995.

[22] G. Cleaver, M. Cvetič, J. R. Espinosa, L. Everett, P. Langacker, and J. Wang, "Physics implications of flat directions in free fermionic superstring models. I. Mass spectrum and couplings," *Physical Review D*, vol. 59, Article ID 055005, 1999.

[23] V. Barger, C.-W. Chianga, P. Langackerb, and H.-S. Leea, "Z′ mediated flavor changing neutral currents in B meson decays," *Physics Letters B*, vol. 580, no. 3-4, pp. 186–196, 2004.

[24] V. Barger, C. W. Chiang, P. Langacker, and H. S. Lee, "Solution to the B $\to \pi$K puzzle in a flavor-changing Z′ model," *Physics Letters B*, vol. 598, no. 3-4, pp. 218–226, 2004.

[25] C. H. Chen and H. Hatanaka, "Nonuniversal Z' couplings in B decays," *Physical Review D*, vol. 73, Article ID 075003, 2006.

[26] V. Barger, L. L. Everetta, J. Jianga, P. Langackerb, T. Liuc, and C. E. M. Wagner, "$b \to S$ transitions in family-dependent U(1)′ models," *Journal of High Energy Physics*, vol. 2009, no. 12, article 48, 2009.

[27] V. Barger, L. Everett, J. Jiang, P. Langacker, T. Liu, and C. E. M. Wagner, "Family nonuniversal $U(1)'$ gauge symmetries and $b \to s$ transitions," *Physical Review D*, vol. 80, Article ID 055008, 2009.

[28] A. K. Alok, S. Baek, and D. London, "Neutral gauge boson contributions to the dimuon charge asymmetry in B decays," *Journal of High Energy Physics*, vol. 2011, article 111, 2011.

[29] K. Leroux and D. London, "Flavour-changing neutral currents and leptophobic Z' gauge bosons," *Physics Letters B*, vol. 526, no. 1-2, pp. 97–103, 2002.

[30] V. Barger, C.-W. Chiang, J. Jiang, and P. Langacker, "$B_s-\overline{B_s}$ mixing in Z′ models with flavor-changing neutral currents," *Physics Letters, Section B*, vol. 596, no. 3-4, pp. 229–239, 2004.

[31] X. G. He and G. Valencia, "$B_s - \overline{B}_s$ mixing constraints on FCNC and a nonuniversal Z'," *Physical Review D*, vol. 74, Article ID 013011, 2006.

[32] C. W. Chiang, N. G. Deshpande, and J. Jiang, "Flavor changing effects in family nonuniversal Z′ models," *Journal of High Energy Physics*, vol. 2006, no. 8, article 75, 2006.

[33] S. Baek, J. H. Jeon, and C. S. Kim, "$B_S^0-\overline{B}_S^0$ mixing in leptophobic Z′ model," *Physics Letters B*, vol. 641, no. 2, pp. 183–188, 2006.

[34] A. Cordero-Cid, G. Tavares-Velasco, and J. J. Toscano, "Effects of an extra Z' gauge boson on the top quark decay $t \to c\gamma$ gamma," *Physical Review D*, vol. 72, Article ID 057701, 2005.

[35] C. X. Yue, H. J. Zong, and L. J. Liu, "Non-universal gauge bosons Z' and rare top decays," *Modern Physics Letters A*, vol. 18, no. 31, pp. 2187–2193, 2003.

[36] K. Y. Lee, S. C. Park, H. S. Song, and C. Yu, "Probing the Z′ gauge boson with the spin configuration of top quark pair production at future e^-e^+ linear colliders," *Physical Review D*, vol. 63, no. 9, Article ID 094010, 2001.

[37] C. X. Yue and L. N. Wang, "Non-universal gauge boson Z' and the spin correlation of top quark pair production at e^-e^+ colliders," *Journal of Physics G: Nuclear and Particle Physics*, vol. 34, no. 1, p. 139, 2007.

[38] F. del Aguila, J. A. Aguilar-Saavedra, M. Moretti, F. Piccinini, R. Pittau, and M. Treccani, "Combined analysis of $Z' \to t\bar{t}$ and $Z' \to t\bar{t}\,j$ production for vector resonance searches at LHC," *Physics Letters B*, vol. 685, no. 4-5, pp. 302–308, 2010.

[39] M. Bobrowski, A. Lenz, J. Riedl, and J. Rohrwild, "How much space is left for a new family of fermions?" *Physical Review D—Particles, Fields, Gravitation and Cosmology*, vol. 79, no. 11, Article ID 113006, 2009.

[40] A. Belyaev, N. D. Christensen, and A. Pukhov, "CalcHEP 3.4 for collider physics within and beyond the Standard Model," *Computer Physics Communications*, vol. 184, no. 7, pp. 1729–1769, 2013.

[41] J. Pumplin, D. R. Stump, J. Huston, H.-L. Lai1, P. Nadolsky, and W.-K. Tung, "New generation of parton distributions with uncertainties from global QCD analysis," *Journal of High Energy Physics*, vol. 2002, no. 7, p. 12, 2002.